Resonance parameter and covariance evaluation for ^{16}O up to 6 MeV

Luiz Leal, Evgeny Ivanov, Gilles Noguere, Arjan Plompen, Stefan Kopecky

EPJ Nuclear Sci. Technol. **2**, 43 (2016)

DOI: 10.1051/epjn/2016036

EPJ Nuclear Sciences & Technologies

Available online at:
http://www.epj-n.org

REGULAR ARTICLE OPEN ACCESS

Resonance parameter and covariance evaluation for ^{16}O up to 6 MeV

Luiz Leal[1,*], Evgeny Ivanov[1], Gilles Noguere[2], Arjan Plompen[3], and Stefan Kopecky[3]

[1] Institut de Radioprotection et de Sûreté Nucléaire (IRSN), PSN-EXP/SNC, 92262 Fontenay-aux-Roses, France
[2] CEA, DEN, DER Cadarache, 13108 Saint Paul les Durance, France
[3] European Commission, Joint Research Centre, Institute for Reference Materials and Measurements, Retieseweg 111, 2440 Geel, Belgium

Received: 6 June 2016 / Received in final form: 5 September 2016 / Accepted: 11 October 2016

Abstract. A resolved resonance evaluation was performed for ^{16}O in the energy range 0 eV to 6 MeV using the computer code SAMMY resulting in a set of resonance parameters (RPs) that describes well the experimental data used in the evaluation. A RP covariance matrix (RPC) was also generated. The RP were converted to the evaluated nuclear data file format using the R-Matrix Limited format and the compact format was used to represent the RPC. In contrast to the customary use of RP, which are frequently intended for the generation of total, capture, and scattering cross sections only, the present RP evaluation permits the computation of angle dependent cross sections. Furthermore, the RPs are capable of representing the (n, α) cross section from the energy threshold (2.354 MeV) of the (n, α) reaction to 6 MeV. The intent of this paper is to describe the procedures used in the evaluation of the RP and RPC, the use of the RPC in benchmark calculations and to assess the impact of the ^{16}O nuclear data uncertainties in the calculate dk_{eff} for critical benchmark experiments.

1 Introduction

Numerous applications in the nuclear data field depend upon a good knowledge and understanding of nuclear data for oxygen. Reactor analysis and design, nuclear criticality safety are among applications for which accurate cross section data and their uncertainties are needed. The processing and disposal of nuclear waste will require a good knowledge of the ^{16}O data and uncertainties. For instance, nuclear spent fuel and waste resulting from reactor power plants are largely in the form of uranium dioxide. In addition the elastic cross section for oxygen is important for fast neutron transport in water moderating system and the (n, α) cross section is important for the production of tritium in the nuclear fuel. In parallel to the present ^{16}O evaluation other evaluation efforts are underway as part of a combined effort, named Collaborative International Evaluated Library Organization also referred to as the (CIELO) project [1]. The main objective of the CIELO ^{16}O evaluation is to investigate issues in connection with the thermal elastic scattering cross section, elastic scattering in the energy 100 keV to 1 MeV, and the (n, α) cross section.

The purpose of this paper is to briefly describe the procedures used in the evaluation of the ^{16}O cross section using the computer code SAMMY [2] from 1.0^{-5} eV up to 6 MeV. The results of the evaluation are a set of RP that reproduces well the experimental data and an RPC that reflects the data uncertainties and correlations.

The motivation for representing the ^{16}O cross-section data with RP came about the time when a SAMMY evaluation of the silicon isotopes was taking place [3]. Among the data used in the silicone evaluation there were data from measurements of enriched silicon samples for ^{28}Si, ^{29}Si, and ^{30}Si in the form of silicon dioxide, that is, $^{28}SiO_2$, $^{29}SiO_2$, and $^{30}SiO_2$. Consequently, there existed the need for RP for oxygen to complete the RP evaluation for silicon. Since no Reich–Moore RP for ^{16}O were available, a provisional set of RP for ^{16}O was derived for the evaluation of the silicon dioxide data up to 1.8 MeV. As the oxygen RP replicated the experimental total cross section for ^{16}O rather well, a full evaluation with the Reich–Moore formalism appeared to be within reach. Therefore, a decision was made to extend the ^{16}O resonance evaluation up to the energy threshold of the first inelastic channel at about 6.049 MeV. However, since it was observed that an (n, α) channel opens about 2.35 MeV, it was required modifying the code SAMMY to account for charged particle penetrability. Sayer [4], together with the author of the SAMMY code, made that option available for fitting charged particle reactions. The charged-particle

* e-mail: luiz.leal@irsn.fr

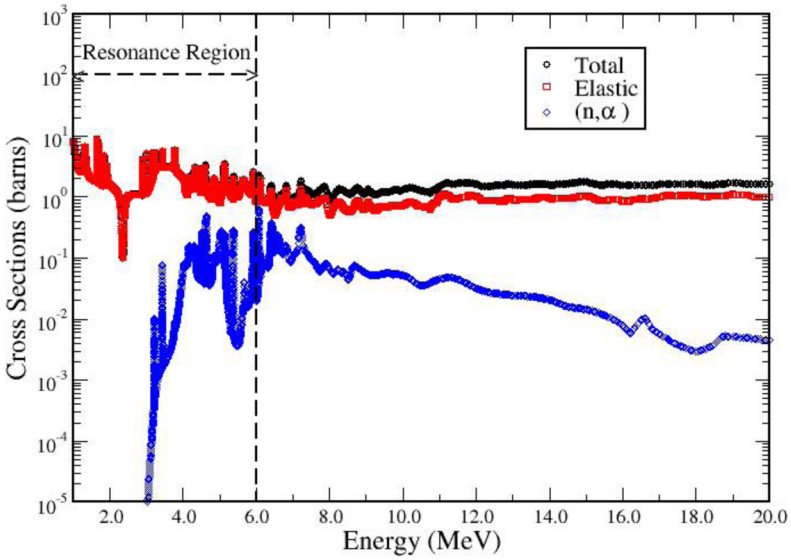

Fig. 1. Total, elastic scattering and (n, α) cross section from ENDF/B-VII.1.

penetrability in SAMMY was exhaustively tested at CEA/Cadarache [5]. Therefore, for the first time a resonance parameter (RP) evaluation for ^{16}O based on the Reich–Moore formalism [6] was completed. Later on Sayer [4] improved the RP evaluation including additional experimental data. It should be pointed out that no RP covariance data were derived at the time the evaluation was done. Other fitting codes such as REFIT [7,8] and CONRAD [9] may be used in the ^{16}O cross section evaluation up to 6 MeV as long as charged-particle penetrability can be calculated.

An example of the total, elastic scattering, and (n, α) cross-sections are shown in Figure 1 calculated from evaluated nuclear data file (ENDF)/B-VII.1.

The issues that prevented proposing the RPs for inclusion in the Evaluated Nuclear Data Libraries, in particular the ENDF library [10], were that the ENDF format could not accommodate charged particle reaction representation using the Reich–Moore formalism. In addition, no existing ENDF processing software such as NJOY [11], AMPX [12], and PREPRO [13] could calculate charged particle penetrability and consequently would not be able to process the evaluation. Therefore, the evaluation did not receive much attention as an option for the ENDF cross-section representation of ^{16}O. Existing evaluations rely entirely on a tabular representation of the data including the angular distribution. Later on the ENDF format was updated to allow the inclusion of more channels and a new resonance format was developed and the cross section processing codes were updated. The ENDF option for representing the RP is named LRF = 7 which is often referred to as the R-Matrix Limited (RML) format. As part of the RP evaluation, a RPC was generated with the code SAMMY. The ENDF format available for representing the covariance matrix for RP in the resolved resonance region is the LCOMP = 1 format, in which the entire covariance matrix is listed. Alternatively, in the LCOMP = 2 format option, the covariance matrix is represented in a compact form, permitting a reduction in the size of the of the covariance matrix. The ENDF representation of the RPC for ^{16}O carried out in the evaluation uses the LCOMP = 2 option.

This paper describes the enhancements and modifications made to the previous resonance evaluation [4] to address issues with energy bound states to represent coherent scattering data, the addition of new thermal capture experimental measurements, use of new total cross section data, fitting of thermal scattering cross section data, and the generation of RPC.

2 Evaluation methodology

2.1 Experimental database

Differential data measurements were used in the SAMMY evaluation of the ^{16}O RP covering the energy range 0–6 MeV. The experimental data used in the evaluation are displayed in Table 1. Four total cross sections were used in the SAMMY evaluation. The SAMMY resonance evaluation of ^{16}O yielded a set of RPs that fit the total, capture at thermal, and the (n, α) cross section in the energy range 0 to 6 MeV. There are 34 resonances in the range 0 to 6 MeV with 3 bound levels and 16 energy levels above 6 MeV for a total of 53 resonances. Up to the (n, α) energy threshold (2.354 MeV) each resonance level is represented by the energy of the resonance E_r, gamma width Γ_γ, and the neutron width Γ_n. Above the threshold an additional channel to represent the (n, α) reaction is added to each energy level with the width Γ_a. The experimental data are well represented with the RPs in conjunction with the Reich–Moore formalism.

Each experimental data was entered sequentially in the fitting process. For a particular SAMMY run an updated set of RP was obtained along with a corresponding RPC. The RP and RPC were entered in a subsequent SAMMY run that generated an improved set of RP and RPC. The process is repeated till a set of RP and RPC reproduces

Table 1. Experimental data used in the ^{16}O evaluation.

Experimental data	Flight-path (m)	Energy range (MeV)	Data reference	Year
Capture cross section	–	Thermal	Firestone [14]	2015
Coherent scattering length	–	–	Sears [15]	1992
Total cross section	79.46	2.0–6.3	ORELA (Larson) [16,17]	1980
Total cross section	249.75	2.0–6.3	RPI (Danon) [18]	2015
Total cross section	41.0 and 47.0	0.6–4.3	ORNL Van de Graaff (Fowler, Johnson, and Feezel) [19]	1973
Total cross section	189.25	3.14–6.3	KFK cyclotron (Cierjacks) [20]	1980
(n, alpha) extracted from (alpha, n)	–	3.2–6.3	ORNL Van de Graaff (Bair and Hass) [21]	1973
(n, alpha) extracted from (alpha, n)	–	3.0–6.3	Tandem Accelerator Universtät Bochum (Harissopulos) [22]	2005

reasonably well all the experimental data analyzed. It should be stressed that the experimental resolutions corresponding to the data shown in Table 1 were correctly entered in the SAMMY fit. There exist available in SAMMY built in resolution functions for the ORELA and RPI machines. For measurements for which a resolution functions are not available SAMMY provides an option for the evaluator to build his own resolution functions, based on Gaussian shape and exponential functions, that suitably fit the data.

2.2 Resonance analysis

The ENDF resonance format that accommodates the Reich–Moore representation (option LRF = 3) of the RPs is restricted to only two channels in addition to the gamma and the elastic channels. To allow the inclusion of additional channels, the RML Format (LRF = 7) was developed in ENDF [10] to allow a much broader use of RPs for reproducing cross sections beyond the usual total, scattering, capture, and fission cross sections. In addition to the full R-matrix representation, all the R-matrix approximations, namely Single Level Breit–Wigner, Multilevel Breit–Wigner, and Reich–Moore formalism, are included in the RML Format.

In the Reich–Moore approach [6], the reduced R-matrix elements are given as

$$R_{cc'} = \sum_{\lambda} \frac{\gamma_{\lambda c}\gamma_{\lambda c'}}{E_\lambda - E - (i\Gamma_{\lambda\gamma}/2)}\delta_{JJ'}. \qquad (1)$$

In this equation the indices c and c' denote the incoming and outgoing channels, respectively. The reduced width amplitudes for the incoming and outgoing channels are, $\gamma_{\lambda c}$ and $\gamma_{\lambda c'}$, respectively. The incident particle energy and the energy eigenvalue, corresponding to the resonance energy, are E and E_λ, respectively while $\delta_{JJ'}$ indicates total momentum conservation. The effect of the gamma channels elimination in the Reich–Moore approximation of the general R-matrix is indicated by the extra term in the denominator of equation (1) that includes the gamma-width amplitude $\Gamma_{\lambda\gamma}$. The appearance of equation (1) is very much like the general R-matrix equation and because of that the Reich–Moore approximation is often referred to as the reduced R-matrix formalism. The Reich–Moore approximation was developed for cross section representation of fissile isotopes for which few fission channels exist and also to account for the interference effect in these channels. However, the Reich–Moore formalism allows the inclusion of additional channels such as the inelastic channels, charged-particle channels, etc. For charged particles, the coulomb effect is taken into account in the shift and penetrability calculations. The charged particle energy dependent shift $S(E)$ and penetrability $P(E)$ are given, respectively, as

$$S(E) = \rho\frac{(F(dF/d\rho)) + (G(dG/d\rho))}{F^2 + G^2}, \qquad (2)$$

and

$$P(E) = \frac{\rho}{F^2 + G^2}. \qquad (3)$$

The functions $F(\rho)$ and $G(\rho)$ are the Coulomb functions where $\rho = ka$ with k the wave number and a the channel radius [23].

Cross-section processing codes such as NJOY [11], AMPX [12], and PREPRO [13] have been updated to accommodate these changes.

Evaluation of the double differential elastic cross section with SAMMY permits reconstruction of the angular distribution of the outgoing particles relative to the incoming particles from the RPs. Angular dependence of the cross section is treated following the Blatt and Biedenharn formalism [24] included in the SAMMY code.

2.3 Energy bound levels

The energy bound levels are used to mock up the effect of the negative resonances in the energy range 0 to 6 MeV. For ^{16}O they are determined according to the excitation energy

levels of the compound nucleus ^{17}O by

$$E_r = \frac{A+1}{A}(E^* - S), \tag{4}$$

where E^* is the energy of the excited states in the compound nucleus, $S = 4.1436$ MeV is the separation energy and $A = 16$. The term $(A+1)/A$ accounts for the center-of-mass to the laboratory system transformation. The energy of the excited states E^*, and the energy bound levels E_r are listed in Table 2 where the spin and parity are denoted by J^π.

Above 6 MeV, sixteen energy levels are needed to account for the interference effects in the energy region 0 to 6 MeV. Figure 2 shows the contribution of the external levels, bound levels and energy level above 6 MeV, in the energy range 0 to 6 MeV. The drop noticed in Figure 2 starting about 500 keV is due to an interference effect in the elastic channels causing a big dip in the total cross section at ∼2.35 MeV where the value is ∼110 mb.

A complete listing of the RPs derived in the evaluation is presented in Table 3. The total angular momentum and parity J^π, angular momentum l, resonance energy E_r, gamma width Γ_γ, neutron width Γ_n, and Γ_α which corresponds to the (n, α) channel are listed.

2.4 Thermal values

Fits of experimental thermal capture and scattering cross sections were obtained by adjusting the neutron and gamma widths of the bound levels. There has been a puzzle as to the value of the thermal scattering cross section that was very well addressed by Lubitz [25]. It is well known that the thermal scattering cross section at zero degree Kelvin at low energy is nearly constant in energy whereas for non-zero temperature a $1/v$ behavior arises. The thermal values quoted in the Atlas of Neutron Resonances [26] are usually at room temperature. However, it appears that for ^{16}O the thermal scattering cross section corresponds to the values calculated in connection with the coherent scattering length determination that is a temperature independent quantity. The actual value of the thermal scattering cross section at room temperature is higher than that corresponding to the coherent scattering length measurements by ∼3%. The discrepancy with the recommended scattering cross section is one of the driving factors for revising the ^{16}O thermal cross section values. The experimental thermal capture cross-section data [14] measured using the activation technique was fitted with SAMMY resulting in a good representation of the data. Results are displayed in Table 4.

Table 2. Energy bound levels for ^{16}O.

E^* (keV)	E_r (keV)	J^π
0.8707	−3477.46	$1/2^+$
3.0554	−1156.20	$1/2^-$
3.843	−319.40	$5/2^-$

2.5 Resonance coherent scattering

In addition to the cross section data, the coherent scattering length [27] was used in the resonance fitting. Without loss of generality, for isolated resonances where no interference effects between resonances are present the coherent scattering length $a_{\rm coh}$ can be defined as [26]

$$a_{\rm coh} = R + \sum_j \frac{\lambda\!\!\!^{-}\,\Gamma_{nj,0}/2}{(E - E_{rj}) + (i\Gamma_j/2)}, \tag{5}$$

where $\Gamma_{nj,0}$ and Γ_j are the reduced neutron width and the total width of the resonance at the energy E_{rj}, respectively, R is the effective scattering radius and $\lambda\!\!\!^{-}$ is related to the wave number k as $k = 2\pi/\lambda\!\!\!^{-}$. Equation (5) is used for $kR \ll 1$, i.e. $E \to 0$. For light nuclides the first resonances are in the keV to MeV range for which the impact on $a_{\rm coh}$ is

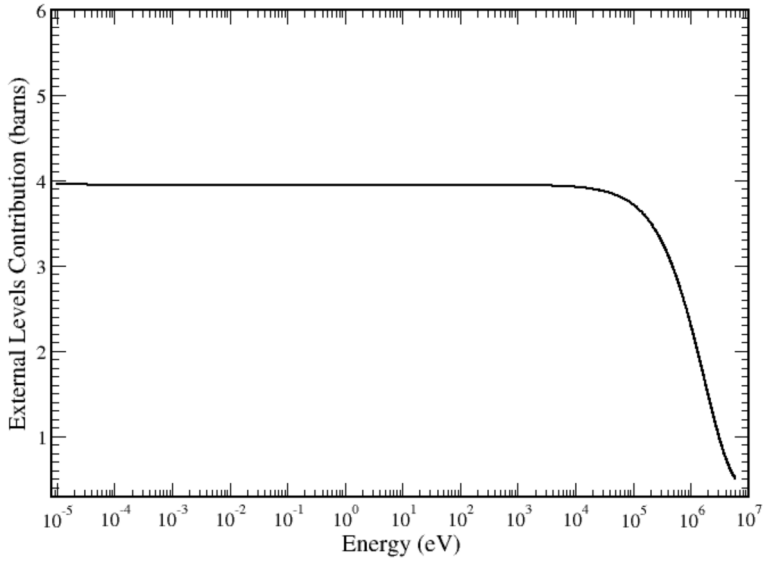

Fig. 2. External levels contribution to the total cross section in the energy range 0 to 6 MeV.

Table 3. List of resonance parameters.

J^π	l	E_r (keV)	Γ_γ (eV)	Γ_n (eV)	Γ_α (eV)
$1/2^+$	0	−3477.46	0.1796	3,897,800.0	
$1/2^-$	1	−1156.20	0.2837	28,406.00	
$5/2^-$	3	−319.40	0.3355	44.361	
$3/2^-$	1	434.10	2.70	44,216.0	
$3/2^+$	2	999.69	0.25	95,884.0	
$3/2^-$	1	1308.30	0.25	43,949.0	
$7/2^-$	3	1650.60	0.25	4049.40	
$5/2^-$	3	1689.30	0.25	145.42	
$3/2^+$	2	1833.50	0.25	7268.40	
$1/2^-$	1	1899.50	0.25	34,406.00	
$1/2^\mp$	0	2367.80	0.25	144,780.00	
$5/2^\mp$	2	2888.50	0.25	459.15	
$7/2^-$	3	3007.11	0.25	43.741	
$5/2^-$	3	3211.70	0.25	1747.70	6.42
$3/2^+$	2	3286.60	0.25	321,580.00	159.62
$5/2^+$	2	3438.50	0.25	480.66	14.97
$5/2^-$	3	3441.50	0.25	1525.80	8.39
$3/2^-$	1	3485.30	0.25	714,150.00	18.32
$7/2^-$	3	3767.00	0.25	18,318.00	19.55
$1/2^-$	1	3974.11	0.25	281,220.00	15,575.00
$1/2^\mp$	0	4054.11	0.25	104,560.00	4305.89
$3/2^+$	2	4177.79	0.25	88,858.00	8907.00
$3/2^-$	1	4298.80	0.25	58,003.00	5130.29
$1/2^-$	1	4312.40	0.25	42,549.00	477.34
$1/2^\mp$	0	4466.10	0.25	13,170.00	2980.20
$5/2^+$	2	4527.11	0.25	4933.22	772.03
$7/2^+$	4	4595.21	0.25	1369.22	288.58
$5/2^-$	3	4631.12	0.25	3051.31	4866.23
$3/2^-$	1	4817.21	0.25	61,269.31	2235.15
$3/2^+$	2	5064.55	0.25	83,638.31	36,080.25
$7/2^-$	3	5124.23	0.25	22,001.14	2042.33
$1/2^-$	1	5311.12	0.25	323.22	594.94
$5/2^+$	2	5368.62	0.25	3129.61	861.45
$3/2^-$	1	5567.89	0.25	20,0320.16	324.67
$5/2^-$	3	5672.31	0.25	282.16	16,169.15
$7/2^+$	4	5918.71	0.25	18,299.32	3327.87
$3/2^-$	1	5992.34	0.25	15,573.12	91.46
$9/2^+$	4	6074.81	0.25	3249.13	2538.55
$1/2^-$	1	6085.23	0.25	19,668.23	1489.81
$7/2^+$	4	6332.21	0.25	3505.39	235,920.21
$7/2^-$	3	6400.29	0.25	43,808.21	38,191.32
$3/2^+$	2	6578.25	0.25	154,720.81	114,320.23
$5/2^-$	3	6672.71	0.25	1864.81	24,775.23
$5/2^+$	2	6740.79	0.25	5032.22	175,840.45
$5/2^+$	2	6786.14	0.25	12,026.32	302,300.11
$7/2^-$	3	6815.22	0.25	19,703.22	36,869.55
$7/2-$	3	7168.70	0.25	308,729.97	223,850.13
$5/2^+$	2	7198.39	0.25	7856.89	19,698.65
$1/2^-$	1	7294.23	0.25	26,161.74	5386.55
$1/2^-$	1	7373.31	0.25	1888.32	
$3/2^-$	1	11,132.00	0.25	17,993,000.00	
$3/2^+$	2	217,224.23	0.25	1,520,600.00	
$1/2-$	1	119,027.00	0.25	34,781,012.00	

Table 4. Thermal values and coherent scattering.

Quantity	Present evaluation (barns) $T' = 0$ K	Present evaluation (barns) $T = 293.6$ K	Experimental (barns)	ANR [24] (barns)	ENDF/B-VII.1 (barns) $T = 0$ K
σ_γ		$(1.67 \pm 0.031) \times 10^{-4}$	$(1.67 \pm 0.023) \times 10^{-4}$ [10]	$(1.9 \pm 0.19) \times 10^{-4}$	1.93×10^{-4}
σ_s	3.765 ± 0.025	3.884 ± 0.022		3.761 ± 0.006	3.852
R'	4.15 ± 0.12 fm			4.8 ± 0.1 fm	5.56 fm
a_{coh}	5.801 ± 0.005 fm		5.803 ± 0.004 fm [11]	5.805 ± 0.005 fm	
I_γ		$(3.09 \pm 0.42) \times 10^{-4}$		$(2.7 \pm 0.3) \times 10^{-4}$	

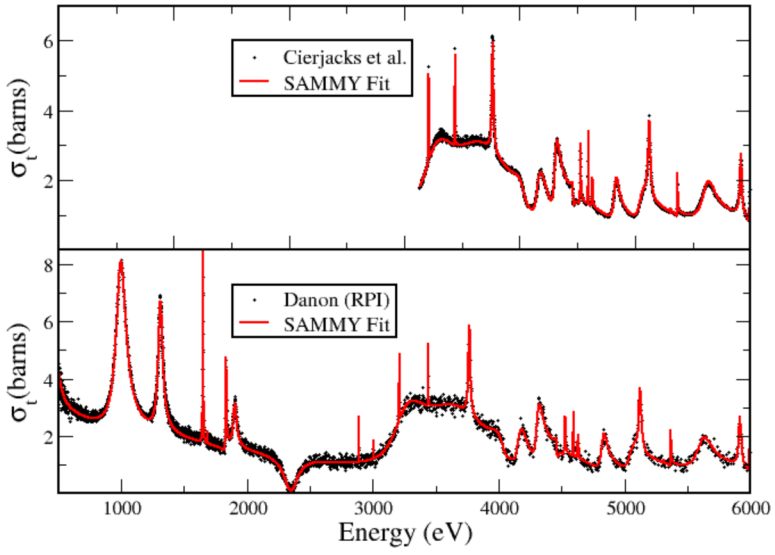

Fig. 3. SAMMY fits for the ^{16}O total cross section of Danon (bottom curve) and Cierjacks et al. (upper curve).

negligible. In contrast, the energy bound states (the negative levels) play an important role in determining a_{coh}. Indeed, the bound levels will guide, in the data evaluation process at low energy, the determination of the thermal scattering cross section, the effective scattering radius R, and the coherent scattering length a_{coh}. Although the derivation above was done on the basis of the SLBW formalism, it is perfectly valid for low mass nuclide at low energy since the resonances interference effects are absent due to the large level spacing. The fitting of the coherent scattering data has not yet been formally implemented in the SAMMY code. However, the experimental scattering length data were fitted with a tool developed outside the SAMMY code environment.

It is interesting to note that the spin coherent and incoherent scattering length, as a function of the spin-dependent scattering lengths a^- and a^+ can be written as

$$a_{\text{coh}} = \frac{I+1}{2I+1} a^+ + \frac{I}{2I+1} a^-, \tag{6}$$

and

$$a_{\text{incoh}} = \frac{[I(I+1)]^{1/2}}{2I+1} (a^+ - a^-), \tag{7}$$

where I is target spin, and that for ^{16}O for which the target spin is zero (i.e., $I = 0$) no incoherent spin scattering exist. Coherent scattering experimental data, taken from reference [15], were used in the evaluation. Results of thermal capture cross-section, effective scattering radius, coherent scattering length and resonance integral obtained by fitting the experimental data are displayed in Table 4. The uncertainties included in the values presented in Table 4 derived in this work are generated from the RP covariance obtained from the resonance analysis of the experimental data that will be discussed later on. Table 4 indicates that the ENDF/B-VII.1 thermal elastic cross section is about 2.3% higher than that derived with the resonance evaluation described in this work. The impact of the lower thermal scattering cross section is addressed in Section 5.

2.6 Cross section fitting

Several experimental data sets were used in the SAMMY fit. As an example, Figure 3 shows a comparison of SAMMY fits with the total cross section of Danon et al. [18] measured at the RPI linear accelerator [28] (bottom curve) and the total cross section of Cierjacks et al. [20]. In Figure 4, a comparison of the differential elastic scattering

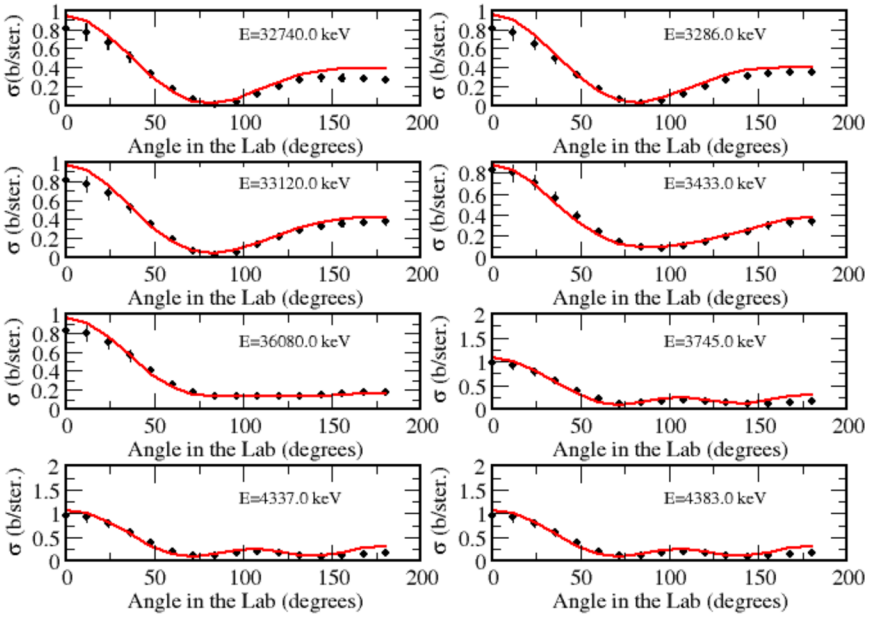

Fig. 4. SAMMY fits for the ^{16}O differential elastic cross section of Lister and Sayers.

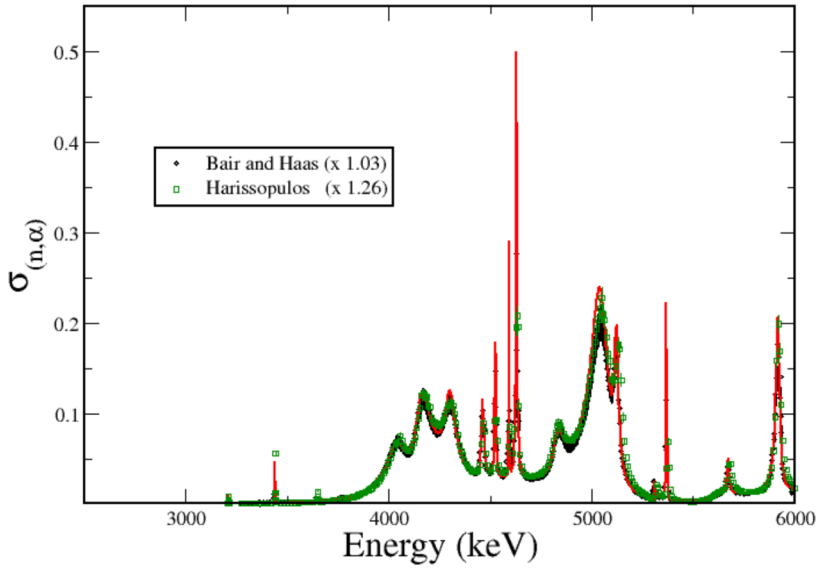

Fig. 5. SAMMY fits of the (n, α) cross sections of Bair and Haas and Harissopulos.

data of Lister and Sayers [29] for energies in the range 3–4 MeV are shown. A good representation of the experimental data with the RPs is obtained.

Another issue investigated in the present work concerns to the (n, α) cross-section. Presently (n, α) cross sections derived from experiments can differ by as much as 30% [30]. To examine the impact of the different (n, α) cross sections in benchmark calculations two sets of RPs were generated based on lower and higher values of the (n, α) cross-sections. Experimental cross section values derived from the corresponding experimental data of Harissopulos et al. [22] ^{13}C(α, n) data were used for the lower cross section value. The (n, α) cross section of Bair and Haas [21] derived from the experimental data for the^{13}C(α, n) reaction were used for the higher cross-section value. Both the lower and the higher cross-section values were fitted with the code SAMMY using the Reich–Moore formalism including the (n, α) channels. The results by fitting the Bair and Haas data are in much better agreement with the total cross section data of Danon et al. with a SAMMY normalization factor of 1.03 for the Bair and Haas data. However, the Harissopulos et al. data require a normalization factor of 1.26 for consistency with Danon's data. The data and the SAMMY fit are displayed in Figure 5. The normalization factors of the total cross sections in Table 1 are in the range of 0.9978 and 1.041.

One may argue that the unitary characteristic of the R-matrix will not be effective due to the (n, γ) channel elimination via the use of the Reich–Moore formalism. It is, however, an integral part of the Reich–Moore approximation that the total cross section is not affected and that the

eliminated capture channel follows the difference between the total cross section and the remaining cross-sections. As a result, the calculated capture cross-sections observe unitarity and typically excellent results are obtained using the Reich–Moore approximation on nuclides with very substantial capture cross-sections. For the present case the capture width and ensuing cross section are small and this point does not warrant further discussion.

The impact of the lower and higher values of the (n, α) cross-sections is investigated in Section 4.

3 Resonance parameter covariance generation

The search for the best set of RPs that fitted the experimental data was carried out in SAMMY with the generalized least-squares method also known as the Bayes' approach. As described in the SAMMY manual [2], if P is the initial guess of the RP with the associated theoretical value T and covariance matrix M, respectively, an updated set of RPs P' and an updated covariance matrix M' are obtained with the equations,

$$(M')^{-1} = M^{-1} + G^t V^{-1} G, \tag{8}$$

and

$$P' = P + M' G V^{-1} (D - T), \tag{9}$$

where D represents the experimental data, V relates to the uncertainties in the experimental data, and G is the sensitivity matrix of the theory with respect to a parameter in P. The matrix V encompasses the statistical and systematical data uncertainties. The SAMMY fitting of the experimental data shown in Table 1 determined the uncertainties and RPC.

The RPC format used to store the information in ENDF was the LCOMP = 2 for which 30% less computer storage is required in comparison with the LCOMP = 1 option with no loss of information.

An example of the RPC for the total cross section is shown in Figure 6 for which the relative uncertainty and correlation are displayed. The results are obtained on calculations done with the PUFF module of the AMPX code [12] with 44-neutron groups. As can be seen below 100 keV the uncertainties in the total cross section are about 1.2%. Above 100 keV, where the contribution due to the resolved resonances starts, the fitting of the experimental data leads to group uncertainties that oscillate reaching out as high as 6%. The 6% uncertainty occurs at the energy corresponding to a minimum of the total cross section meaning that a small cross-section infers a higher uncertainty.

Another example is the uncertainty in the (n, α) cross sections, which is shown in Figure 7.

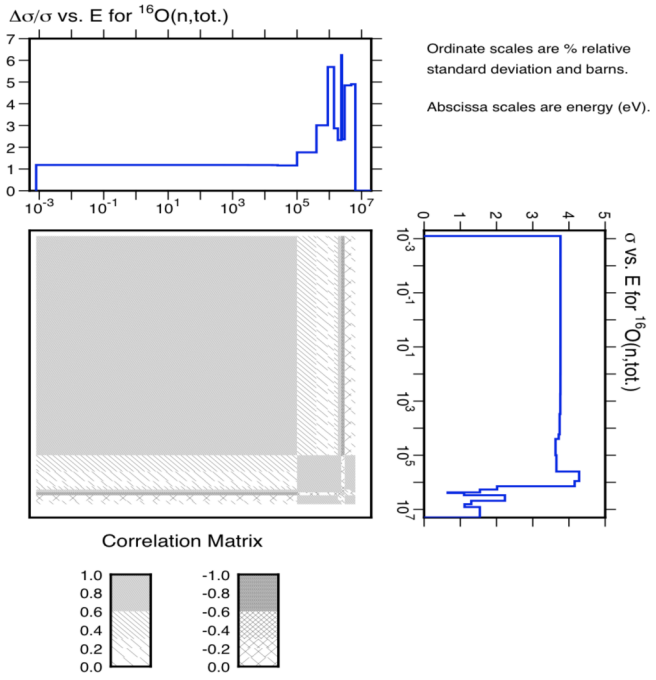

Fig. 6. Correlation matrix for the total cross section up to 6 MeV.

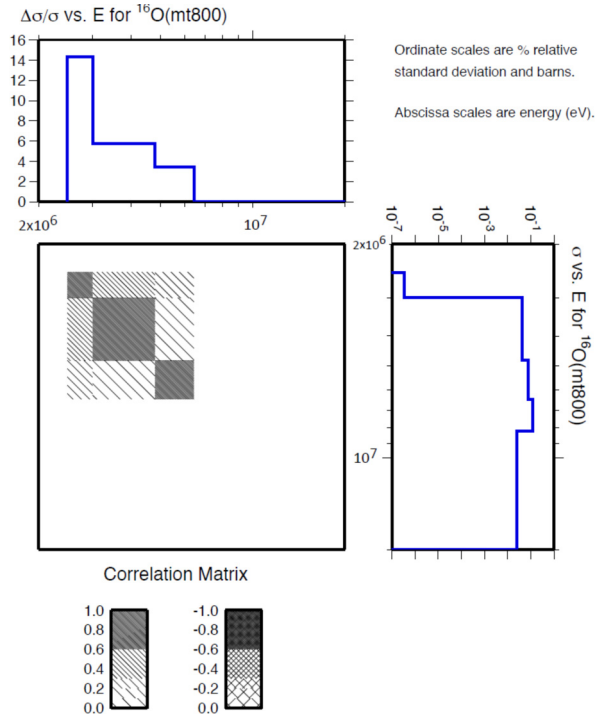

Fig. 7. Correlation matrix for the (n, α) cross section up to 6 MeV.

4 Benchmark studies

The ^{16}O scattering cross section at thermal energy derived in the present evaluation at room temperature is lower by 2.5% compared with the values in existing nuclear data libraries. In this session the impact of the low scattering cross-section in benchmark calculations is investigated. Moreover, comparisons of benchmark results using two sets of the ^{16}O (n, α) cross-section values corresponding to the fitting of two experimental data, that is low and high, are also presented.

Table 5. Benchmark results.

Benchmark	A ENDF/B-VII.1	B Low	C High	Benchmark k_{eff}
LEU-MET-THERM-015-15	1.00533 ± 0.00052	1.00351 ± 0.00050	1.00311 ± 0.00052	1.0000 ± 0.0051
LEU-MET-THERM-015-16	1.00549 ± 0.00052	1.00344 ± 0.00052	1.00242 ± 0.00052	1.0000 ± 0.0051
ZED-2	0.99866 ± 0.00018	0.99833 ± 0.00019	0.99772 ± 0.00019	1.0035 ± 0.0035

Prior using the evaluated RPs in benchmark calculations the SAMMY RPs were converted into the ENDF LRF = 7 format. The ENDF/B-VII.1 ^{16}O evaluation was used as the base library. The ^{16}O ENDF LRF=7 RPs were inserted in the ENDF/B-VII.1 for calculation of the cross section in the energy range of 10^{-5} eV to 6 MeV. One should bear in mind that in addition to the energy dependent cross section angular data are also retrieved from the RPs. Above 6 MeV, the ENDF cross section values are used. The evaluations were processed with the NJOY code, the NJOY2012.50 adapted to retrieve angular data from RP, and the benchmark calculations were done with the MCNP code [31].

Three benchmarks, namely two light-enriched and light-water moderated and one light-enriched and heavy-water moderated systems, extracted from the International Criticality Safety Benchmark Evaluation Project (ICSBEP) [32] named LEU-MET-THERM-015 cases 15 and 16 and another from the International Reactor Physics Experiments Evaluation [33] named Zero Energy Deuterium Reactor first case, were used in the MCNP calculations. The heavy water critical benchmark systems was chosen since the sensitivity to ^{16}O cross sections is enhanced due to the small step of the neutron energy slowing in the heavy water. The k_{eff} results are shown in Table 5 including the statistical error in connection with the Monte Carlo sampling. The experimental benchmark values and experimental uncertainty are listed in the far right column. The nuclear data for the remaining isotopes present in the benchmark were that of the MCNP library based on the ENDF/B-VII.1. The MCNP results corresponding to the ENDF/B-VII.1 data are shown in column A whereas the results for the low and high (n, α) cross-sections are shown in column B and C, respectively. It is noted a considerable decrease in the k_{eff} values from column A compared with values indicated in column B and C. The decrease in k_{eff} from column A to B is due to a decrease on the elastic scattering cross section. This result is in agreement with the suggestion made by Lubitz's [25] that the scattering cross section should be lowered for about 3% from the existing values in the evaluated nuclear data files. The impact on the magnitude of the (n, α) cross-section data in the k_{eff} results can be seen on columns B and C. It seems that the impact of the low to high (n, α) cross-sections is not a very big improvement in the k_{eff} results. More benchmark calculations should be performed with system sensitive to the (n, α) cross-sections to better understand the effect of the new RPs evaluation on integral benchmark calculations. However the results presented in this work demonstrate that the new evaluation is performing reasonably well.

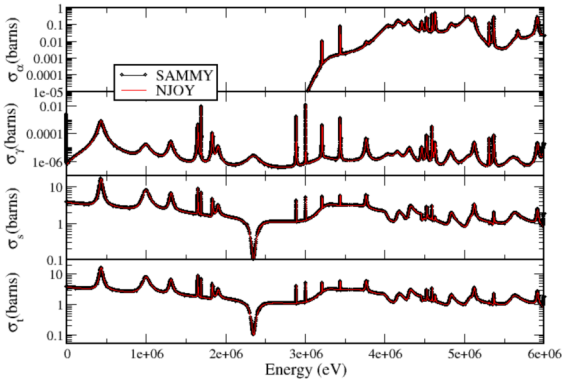

Fig. 8. NJOY and SAMMY computed cross sections corresponding to the high (n, α).

Comparisons of the total capture, scattering, and (n, α) cross sections processed with NJOY and the SAMMY code corresponding to the high (n, α) are shown in Figure 8. In general the percentage difference between the two-processed NJOY-SAMMY cross sections ranges around 10^{-5}%.

A comparison of the shape of the low and high the (n, α) cross-sections, processed with SAMMY, is displayed in Figure 9 in which the difference in the cross section can be observed. Below 6 MeV the magnitude of the (n, α) cross-section is small in comparison with the total cross section. Figure 10 shows the low and high total cross sections (top curve) and the relative difference in absolute value (bottom curve).

5 Uncertainty propagation of the ^{16}O covariance data on benchmark calculations

Uncertainty on k_{eff} due to the nuclear data are commonly carried out based on a first order approximation that translates into the following equation

$$\text{var}(k_{\text{eff}}) = \text{S}_k \cdot \text{C} \cdot \text{S}_k^T, \tag{10}$$

where $\mathbf{C}$ is the nuclear data covariance and $\mathbf{S}_k$ the sensitivity, which provides an indication of the cross section changes and the corresponding effects on k_{eff}, is defined as

$$\text{S}_k = \frac{\sigma}{k_{\text{eff}}} \cdot \frac{\partial k_{\text{eff}}}{\partial \sigma}. \tag{11}$$

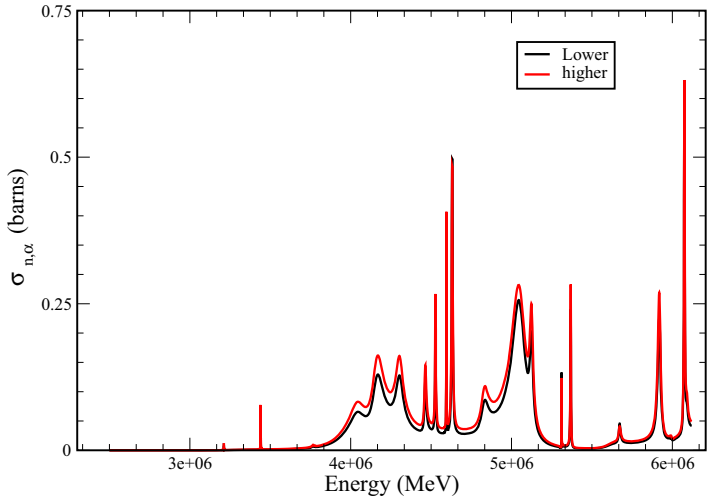

Fig. 9. Shape of the low and high $^{16}O(n, \alpha)$ cross-section.

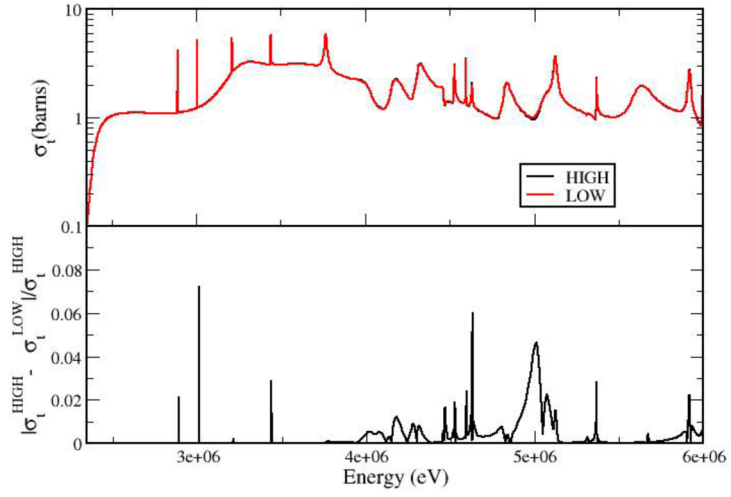

Fig. 10. Total low and high cross sections (top curve) and the relative difference in absolute value (bottom curve).

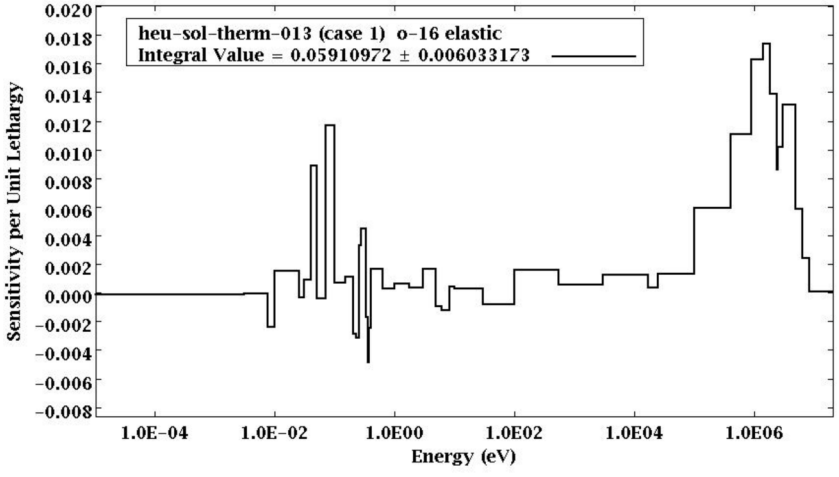

Fig. 11. 44-group MCNP calculated elastic cross-section sensitivity.

Table 6. Benchmark result.

Benchmark	Benchmark k_{eff}	ENDF/B-VII.1 (C1)	ENDF/B-VII.1 + new^{16}O (HIGH) (C2)	C2−C1 (pcm)
HEU-SOL-THERM-013 (Case 1)	1.0012 ± 0.0026	0.99862 ± 0.00011	0.99719 ± 0.00011	−143
HEU-SOL-THERM-013 (Case 2)	1.0007 ± 0.0036	0.9975 ± 5.00012	0.99627 ± 0.00012	−149
HEU-SOL-THERM-013 (Case 3)	1.0009 ± 0.0036	0.99410 ± 0.00013	0.99261 ± 0.00013	−149
HEU-SOL-THERM-013 (Case 4)	1.0003 ± 0.0036	0.99608 ± 0.00013	0.99427 ± 0.00013	−181

Q6 **Table 7.** Uncertainty propagation on k_{eff} due to nuclear data uncertainty.

k_{eff}	% $dk_{\text{eff}}/k_{\text{eff}}$	Individual contributions		
		HEU-SOL-THERM-013 (Case 1)		
		(n, n)	(n, n)	0.140440 ± 0.00364
		(n, γ)	(n, n)	0.060989 ± 0.00058
0.99719 ± 0.00011	0.15730 ± 0.00368	(n, α)	(n, α)	0.023915 ± 0.00004
		(n, γ)	(n, γ)	0.023341 ± 0.00003
		(n, n)	(n, α)	0.013680 ± 0.00004
		HEU-SOL-THERM-013 (Case 2)		
		(n, n)	(n, n)	0.116510 ± 0.00400
		(n, γ)	(n, n)	0.056059 ± 0.00007
0.99627 ± 0.00012	0.13420 ± 0.00407	(n, α)	(n, α)	0.023943 ± 0.00004
		(n, γ)	(n, γ)	0.023408 ± 0.00004
		(n, n)	(n, α)	0.012662 ± 0.00005
		HEU-SOL-THERM-013 (Case 3)		
		(n, n)	(n, n)	0.158180 ± 0.00430
		(n, γ)	(n, n)	0.065152 ± 0.00057
0.99621 ± 0.00013	0.17480 ± 0.00434	(n, α)	(n, α)	0.023779 ± 0.00003
		(n, γ)	(n, γ)	0.023297 ± 0.00003
		(n, n)	(n, α)	0.013251 ± 0.00004
		HEU-SOL-THERM-013 (Case 4)		
		(n, n)	(n, n)	0.140080 ± 0.00407
		(n, γ)	(n, n)	0.061119 ± 0.00059
0.99427 ± 0.00013	0.15680 ± 0.00411	(n, α)	(n, α)	0.023640 ± 0.00004
		(n, γ)	(n, γ)	0.023029 ± 0.00003
		(n, n)	(n, α)	0.011153 ± 0.00004

The uncertainty on k_{eff} due to the nuclear data covariance information provided in the matrix C is accomplished by $\sqrt{\text{var}(k_{\text{eff}})}$.

The effect of the propagation of the uncertainties given by the ^{16}O covariance data on the multiplication factor k_{eff} has been tested for four highly enriched critical benchmark experiments extracted from the ICSBEP [32] using the high (n, α) cross-section. These benchmarks are unreflected spheres identified in the ICSBEP handbook as HEU-SOL-THERM-013 (Case 1), HEU-SOL-THERM-013 (Case 2), HEU-SOL-THERM-013 (Case 3), and HEU-SOL-THERM-013 (Case 4), respectively. They are also referred to as the ORNL spheres benchmarks. The MCNP code was used to compute the sensitivities. As an example, Figure 11 shows the sensitivity of k_{eff} to the elastic cross section of ^{16}O for the HEU-SOL-THERM-013 (Case 1) benchmark.

The MCNP k_{eff} results, including the statistical sample error, using the new ^{16}O evaluation (referred to as HIGH) are shown in Table 5. Also shown in Table 5 is the experimental k_{eff} with the experimental uncertainty. Similar to the procedure used in Section 4 the ENDF/B-VII.1 was used as the reference library. By way of comparisons, Table 6 also illustrates the results of calculationsbased solely on the ENDF/B-VII.1 data. The use of the new ^{16}O evaluation leads

to a reduction on the k_{eff} values about 150 pcm, which is explained on the grounds of the 3% reduction in the scattering cross section. In principle one may dispute that the new evaluation results do not support a good calculation of critical benchmark. However, it should be pointed out that the present ^{16}O evaluation effort is part of the CIELO project [1], aimed at revisiting and improving the evaluations of ^{1}H, ^{56}Fe, and major actinides including ^{235}U, ^{238}U, and ^{239}Pu as part of the project. Hence changes and improvements of the k_{eff} results presented in Table 5 are expected as new evaluations become available mainly for ^{235}U and ^{238}U

The effect of the ^{16}O nuclear data uncertainty propagated to the k_{eff} results has been accomplished by using the TSUNAMI-IP sequence of the SCALE code system [34], which consists of combining the sensitivity and the covariance data to calculate the variance on k_{eff} as spelled out in equation 10. The results are displayed on Table 7 for each of the four-benchmark cases. The first column is the k_{eff}, which is also given in the third column of Table 6. Listed in the third column of Table 7 is the percentage standard deviation of k_{eff} due the nuclear data uncertainties on the ^{16}O cross section. Note that the statistical error resulting from the Monte Carlo sampling is also listed. The last column in Table 7 are the individual nuclear data uncertainty contributions for the (n, n), (n, γ), and (n, α) as well as their correlations. Note that the relative standard deviation in k_{eff} is computed from the individual values by adding the square of the values and taking the square root.

It can be noted that the variations of the k_{eff} lie within the error bars derived from the nuclear data covariance. In all four cases the major contributor to the benchmark uncertainty, only due to the ^{16}O covariance data, is from the (n, n) reaction. Indeed, the (n, n) represents ~90% of the total ^{16}O uncertainty.

6 Conclusions

This paper depicts a certain degree of detail the work done in the resonance evaluation of ^{16}O cross section in the energy range 0 to 6 MeV using the reduced Reich–Moore formalism of the SAMMY code. The procedure used for performing the resolved resonance evaluation, generation of RP covariance, inclusion of the evaluation in the ENDFs, and the processing of the data for use in calculation of k_{eff} is described. Double-differential elastic cross-sections were fitted based on the Blatt and Biedenharn formalism and RP covariance was generated in the fitting process of the experimental data. The evaluation addresses concerns with regard to thermal elastic cross section data and coherent scattering data. Thorough comparisons of the point cross-section generated with the code SAMMY, AMPX, and NJOY was carried out. The paper discusses the issue on the normalization of the (n, α) cross sections from the viewpoint of simple benchmark calculations. The use of the ENDF data representation based on the LRF = 7 and LCOMP = 2 has been discussed. The impact of the nuclear data uncertainty propagation on benchmark calculations was presented based on four highly enriched critical benchmark systems.

For the benchmarks analyzed we observe a systematic decrease in the calculated reactivity of 150 pcm due to the decrease of the elastic scattering cross section. The magnitude of the uncertainty derived from the RPC due to ^{16}O propagated to the benchmark calculation is about 150 pcm.

Part of this work was supported by the United State Department of Energy, Nuclear Criticality Safety Program while L. Leal was an employee of the Oak Ridge National Laboratory.

References

1. M.B. Chadwick, E. Dupont, E. Bauge, A. Blokhin, O. Bouland, D.A. Brown, R. Capoteg, A. Carlson, Y. Danon, C. De SaintJean, M. Dunn, U. Fischer, R.A. Forrest, S.C. Franklea, T. Fukahoril, Z. Gem, S.M. Grimesn, G.M. Halea, M. Hermanf, A. Ignatyukd, M. Ishikawa, N. Iwamoto, O. Iwamoto, M. Jandel, R. Jacqmin, T. Kawano, S. Kunieda, A. Kahler, B. Kiedrowski, I. Kodeli, A.J. Koning, L. Leal, Y.O. Lee, J.P. Lestone, C. Lubitz, M. MacInnes, D. McNabb, R. McKnight, M. Moxon, S. Mughabghab, G. Noguere, G. Palmiotti, A. Plompen, B. Pritychenko, V. Pronyaev, D. Rochman, P. Romain, D. Roubtsovx, P. Schillebeeckxw, M. Salvatorese, S. Simakovg, E.S. Soukhovitskiĭy, J.C. Sublet, P. Talou, I. Thompson, A. Trkov, R. Vogt, S. van der Marck, The CIELO collaboration: neutron reactions on ^{1}H, ^{16}O, ^{56}Fe, ^{235,238}U, and ^{239}Pu, Nucl. Data Sheets **118**, 1 (2014)
2. N.M. Larson, *Updated Users' Guide for SAMMY: Multi-level R-Matrix Fits to Neutron Data Using Bayes's Equations*, ENDF-364/R2 (Oak Ridge National Laboratory, USA, 2008), available at Radiation Safety Information Computational Center (RSICC) as PSR-158
3. L.C. Leal, R.O. Sayer, N.M. Larson, R.R. Spencer, *R*-matrix evaluation of ^{16}O neutron cross sections up to 6.3 MeV, in *American Nuclear Society Winter Meeting* (TANSAO, Washington, 1998), Vol. 79, p. 175
4. R.O.Sayer, L.C. Leal, N.M. Larson, R.R. Spencer, R.Q. Wright, *R*-matrix evaluation of ^{16}O neutron cross sections up to 6.3 MeV, ORNL/TM-2000/212, 2000
5. O. Bouland, R. Babut, O. Bersillon, Experimental cross-section data by a SAMMY parameterization: ^{9}B(α, n) cross section evaluation up to 4 MeV, in *International Conference on Nuclear Data for Science and Technology, September 26–October 1, 2004* (American Institute of Physics, Santa Fe, NM, USA, 2005), Vol. 1, p. 418
6. C.W. Reich, M.S. Moore, Multilevel formula for the fission process, Phys. Rev. **111**, 929 (1958)
7. M.C. Moxon, T.C. Ware, C.J. Dean, *REFIT-2009 A Least-Square Fitting Program for Resonance Analysis of Neutron Transmission, Capture, Fission and Scattering Data Users' Guide for REFIT-2009-10* (UKNSFP243, 2010)
8. M.C. Moxon, J.B. Brisland, GEEL REFIT, A least squares fitting program for resonance analysis of neutron transmission and capture data computer code, in *AEA-InTec-0630* (AEA Technology, 1991)
9. P. Archier et al., CONRAD evaluation code: development status and perspectives, in *Proc. of the International Conference on Nuclear Data for Science and Technology, ND2013, New-York, USA* (2013)
10. *ENDF-6 Formats Manual, Formats and Procedures for the Evaluated Nuclear Data Files ENDF/B-VI and ENDF/B-VII*, edited by M. Herman, A. Trkov, Report-BNL-90365-2009 Rev. 1 (National Nuclear Data Center, Upton, NY, 2010)

11. R.E. MacFarlane, D.W. Muir, A.C. Kahler, *The NJOY Nuclear Data Processing System, Version 2012*, LA-UR-12-27079 (Los Alamos National Laboratory, 2012)
12. M.E. Dunn, N.M. Greene, AMPX-2000: a cross-section processing system for generating nuclear data for criticality safety applications, Trans. Am. Nucl. Soc. **86**, 118 (2002)
13. D.E. Cullen, *PREPRO 2015 2015 ENDF/B Pre-processing Codes (ENDF/B-VII Tested)*, IAEA-NDS-39 Rev. 16 (The Nuclear Data Section International Atomic Energy Agency, 2015)
14. R.B. Firestone, EGA status 2015, in *21st Technical Meeting of the Nuclear Structure and Decay Data Network, 20–24 April, 2015* (IAEA, Vienna, 2008)
15. V.F. Sears, Neutron scattering lengths and cross sections, Neutron News **3**, 29 (1992)
16. D.C. Larson, in *Symposium on Neutron Cross Section from 10 to 50 MeV, BNL-NCS-51245* (1980), p. 277
17. D.C. Larson, J.A. Harvey, N.W. Hill, in *Proc. Int. Conf. On Nuclear Cross Sections for Technology, Knoxville* (1980), p. 34
18. Y. Danon, Private communication
19. J.L. Fowler, C.H. Johnson, R.M. Feezel, Phys. Rev. C **8**, 545 (1973)
20. S. Cierjacks, F. Hinterberg, G. Schmalz, D. Erbe, P.B. Rossen, B. Leugers, Nucl. Inst. Meth. **169**, 185 (1980)
21. J.K. Bair, F.X. Haas, Phys. Rev. **C7**, 1356 (1973)
22. S. Harissopulos et al., Cross-section of the ^{13}C(α,n) reaction: a background for the measurement of geo-neutrinos, Phys. Rev. C **72**, 062801 (2005)
23. I.J. Thompson, F.M. Nunes, *Nuclear reactions for astrophysics, principles, calculations and applications of low-energy reaction* (Cambridge University Press, 2009)
24. J.M. Blatt, L.C. Biedenharn, The angular distribution of scattering and reaction cross sections, Rev. Mod. Phys. **24**, 258 (1952)
25. C. Lubitz, P. Romano, T. Trumbull, D. Barry, Evidence for a 3 % 'Doppler-Error' in the ^{16}O neutron cross section database, in *NEMEA-7/CIELO Workshop, November 5–8* (2013)
26. S.F. Mughabghab, *Atlas of neutron resonances − resonance parameters and thermal cross section Z = 1–100* (Elsevier Publisher, Amsterdam, 2006)
27. S. Kopecky, A. Plompen, Low-energy scattering for oxygen, in *NEMEA-7/CIELO Workshop* (NEA/NS/DOC, 2014), Vol. 13, p. 23
28. Y. Danon, R.M. Bahran, E.J. Blain, A.M. Daskalakis, B.J. McDermott, D.G. Williams, D.P. Barry, G. Leinweber, M.J. Rapp, R.C. Block, Nuclear data for criticality safety and reactor applications at the gaerttner LINAC center, Trans. Am. Nucl. Soc. **107**, 690 (2012)
29. D. Lister, A. Sayers, Phys. Rev. **143**, 745 (1966)
30. G.M. Hale, M.W. Paris, Status and plans for ^{1}H and ^{16}O evaluations by *R*-matrix analyses of NN and ^{17}O systems, LA-UR-14-21339, in *Presented at the NEMEA-7/CIELO Workshop, 05–08, November, 2013, Geel, Belgium* (2013)
31. X-5 Monte Carlo Team, *LA-CP-03-0245* (Los Alamos National Laboratory, 2003)
32. International Handbook of Evaluated Criticality Safety Benchmark Experiments, NEA/NSC/DOC(95)/01/1-IX, *Organization for Economics Co-operation and Development* (Nuclear Energy Agency (OECD-NEA), 2013)
33. International Handbook of Evaluated Reactor Physics Benchmark Experiments, NEA/NSC/DOC(2006), *Organization for Economics Co-operation and Development* (Nuclear Energy Agency (OECD-NEA), 2013)
34. SCALE, *A Comprehensive Modeling and Simulation Suite for Nuclear Safety Analysis and Design, ORNL/TM-2005/39, Version 6.1* (Oak Ridge National Laboratory, Oak Ridge, Tennessee, 2011), available from Radiation Safety Information Computational Center at Oak Ridge National Laboratory as CCC-785

Cite this article as: Luiz Leal, Evgeny Ivanov, Gilles Noguere, Arjan Plompen, Stefan Kopecky, Resonance parameter and covariance evaluation for ^{16}O up to 6 MeV, EPJ Nuclear Sci. Technol. **2**, 43 (2016)